The measurement and calculation of birefringence in quenched polycarbonate specimens

R. Wimberger-Friedl and R. D. H. M. Hendriks
Philips Research Laboratories, PO Box 80000, 5600-JA Eindhoven, The Netherlands
(Received 23 November 1988; accepted 9 December 1988)

The stress-induced birefringence in quenched polycarbonate discs is calculated with a numerical program and compared with birefringence measurements. Use is made of a thermo-viscous-elastic model with a discontinuous change of the properties at the glass transition temperature, T_g. The birefringence is calculated with the aid of the stress-optical rule using the measured stress-optical coefficients in the molten and glassy states. The birefringence present at the moment of glass transition is 'frozen in' and added to the birefringence that builds up below T_g. The calculated birefringence distributions fit the distributions measured in cross-sections of the samples. The birefringence distributions are unbalanced because of the contribution of frozen-in orientation, induced by the cooling stresses above T_g. In constrained quenching the contact with the wall leads to high tensile stresses in the melt, which, depending on the adhesion of the polymer to the wall, induce unexpected birefringence distributions.

(Keywords: cooling stresses; birefringence; polycarbonate; stress-optical coefficient; frozen-in orientation)

INTRODUCTION

Dimensional stability of amorphous polymer specimens is determined not only by the non-equilibrium volume relaxation, called physical ageing[1], but also by the presence of internal stresses and orientation of the polymer chains[2]. In injection moulding the polymer undergoes a very complicated stress–strain–temperature course, of which only parts can be described quantitatively[3–5]. Nevertheless, it is this course that determines the frozen-in stresses and orientation distribution in the sample. Therefore it seems desirable to have access to this 'state' of the specimen from two points of view: namely to have a real reference for the measurement of dimensional stability and to be able to verify the results of numerical simulations. The ultimate goal is to predict dimensional stability from numerical simulation of the processing cycle.

The birefringence technique has been successfully applied to the analysis of frozen-in orientation in injection-moulded samples[6,7]. Mostly polystyrene (PS) has been used in such studies. The stress-optical sensitivity of PS in the glassy state is 400 times lower than in the molten state[8,9]. Therefore the contribution of the cooling stresses to the birefringence can be neglected compared to that of the flow-induced stresses[10]. Bisphenol A polycarbonate (PC), however, has a high stress-optical sensitivity above as well as below the glass transition temperature (T_g), as will be shown. Therefore both the frozen-in orientation and the cooling stresses contribute to a comparable extent to the residual birefringence. In order to be able to split these two components one has to quantify one of the contributions. In our investigations we try to quantify the birefringence caused by cooling stresses alone.

For this purpose the stress-optical behaviour and the mechanical properties of PC are determined in the molten and glassy states. Disc-shaped specimens are quenched in a turbulent liquid (free quenching) and in a specially designed apparatus (constrained quenching). The residual birefringence distribution is determined and compared with the results obtained with a numerical program developed for this purpose.

Stress-optical characterization

It has been shown experimentally that in polymer melts the birefringence (Δn) is proportional to the applied stress difference ($\Delta\sigma$):

$$\Delta n = C_m \Delta\sigma \tag{1}$$

This is the well known stress-optical rule[11]. The stress-optical coefficient (C_m) is proportional to the anisotropy of the polarizability of the polymer chain. In the glassy state a linear relation has also been found[8], although it has not yet been derived theoretically. Whereas in the melt the application of a stress difference leads to an orientation of the chain segments, referred to as entropic stress, in the glassy state the intermolecular distances are changed and the chain bonds are distorted locally, referred to as energetic stress. In the glass transition region the timescale of orientation is comparable to a characteristic processing time so that C becomes time-dependent and the linearity of the stress-optical rule is lost. When the melt is cooled through the glass transition in a stressed state the orientation is frozen in.

Birefringence is accessible as the path difference or optical retardation (Γ) of the ordinary and extraordinary beam in the plane perpendicular to the direction of light propagation. For the measurement of the retardation between crossed polarizers the principal directions of the medium have to lie in this plane and the polarizer must be at 45° with respect to the principal directions.

032-3861/89/061143-07$03.00

The standard techniques for the isothermal characterization are uniaxial extension and simple shear. Since the refractive index and stress tensor are coaxial in the isothermal case in uniaxial extension, the draw direction is at 45° with respect to the polarizer. The stress-optical coefficient is calculated as follows:

$$C_g = \Delta n/\sigma_1 \tag{2}$$

where σ_1 is the tensile stress.

Uniaxial extension is difficult to achieve in melts. Therefore the simple shear deformation is used. There one has to be aware of the rotation of the main stresses in the shear plane around the angle X, which depends on the shear rate. The crossed polarizers must be rotated around the neutral direction of the shear flow about that angle. The stress-optical coefficient is then calculated with the aid of the following formula[12]:

$$C_m = \Delta n \sin(2X)/2\sigma_{21} \tag{3}$$

where σ_{21} is the shear stress.

Cooling stresses

The combination of an inhomogeneous temperature distribution and a strong temperature dependence of the mechanical properties leads to a build-up of cooling stresses. This was first observed in inorganic glasses. Aggarwala and Saibel[13] developed an analytical solution by assuming that the viscosity changes from zero to infinity at a certain temperature. Struik[2] and Greener and Kenyon[14] applied this model for polymers. Lee, Rogers and Woo[15] first included viscoelastic behaviour of the glass. Their model was applied to polymers by Wust and Bogue[16] and Lee *et al.*[17]. Since mechanical methods of measurement of internal stresses (the best known technique being layer removal as introduced by Treuting and Read[18]) can be applied successfully only under certain assumptions in simple geometries[19–21], birefringence has become an important alternative. The observed birefringence distributions are not balanced[10,15,22,23] generally because birefringence has, as already mentioned, two different physical origins. Therefore models that either disregard the modulus or viscosity above T_g or make use of a single stress-optical coefficient cannot predict residual birefringence distributions correctly.

When a thin specimen is quenched freely the shrinkage of the surface layer induces compressive stresses in the still soft core. With further penetration of the solidification the incremental layer passes the glass transition in a stressed state. Whether this stress is tensile or compressive depends on the difference in mechanical properties above and below T_g and also on the temperature step that is applied. As every volume element passes the glass transition in the stressed state there will always be a contribution of orientation of the molecules to the residual birefringence distribution. The degree of imbalance of the latter depends on the difference in stress-optical coefficients above and below T_g and the cooling conditions, i.e. the initial temperature.

The situation is different in a constrained quench, when the no-slip condition is applied. There only tensile stresses develop. Only after the sample is released from the wall will the stresses equilibrate within the sample. Ultimately a very flat birefringence and stress distribution is obtained, as observed with polystyrene by Isayev[10].

In the present investigation we calculate the stress build-up during cooling and make use of the stress-optical rule in the molten and glassy states with the respective stress-optical coefficients determined experimentally.

THE NUMERICAL SIMULATION PROGRAM

A numerical program was developed in order to study the build-up of cooling stresses in circularly symmetric samples during rapid cooling. The program makes use of the finite element method[24] and is incorporated in the commercial program package SEPRAN*. The equations for the balance of mass, momentum and energy are simplified by the following assumptions: inertia, gravity and dissipation of mechanical energy can be disregarded and there is no energy source present. This yields the following set of equations:

$$\nabla\cdot\boldsymbol{\sigma}=\mathbf{0} \qquad \dot{v}/v-\nabla\cdot\boldsymbol{u}=\mathbf{0} \qquad \text{and} \qquad \dot{e}/v=-\nabla\boldsymbol{h} \tag{4}$$

To these balance equations are added the constitutive equations, which describe the material behaviour:

$$\dot{e}=c_p\dot{T} \qquad \boldsymbol{h}=-\lambda(\nabla T)$$
$$v=[v_0+v_0\alpha(T-T_g)](1-p/\kappa) \tag{5}$$
$$\boldsymbol{\sigma}(t)=-p(t)\boldsymbol{I}+\boldsymbol{\tau}(t)$$

with

$$\boldsymbol{\tau}(t)=2\eta(T)\boldsymbol{D}^d(t) \qquad \text{for all } T>T_r$$
$$\boldsymbol{\tau}(t)=2G_r\int_{s=t_r}^{t}\boldsymbol{D}^d(s)\,ds \qquad \text{for all } T_g<T<T_r \tag{6}$$
$$\boldsymbol{\tau}(t)=\boldsymbol{\tau}(t_g)+2G_g\int_{s=t_g}^{t}\boldsymbol{D}^d(s)\,ds \qquad \text{for all } T<T_g$$

The dots represent the time derivative and T_r is the transition temperature from viscous to rubber-elastic material behaviour. The method of weighted residuals is applied to equations (4). Temporal discretization is performed by applying implicit Euler time stepping. For the spatial discretization, use is made of a seven-node Taylor–Hood element[25], shown in *Figure 1*. Circular symmetry is assumed. The resulting set of non-linear equations is solved by the Picard iteration scheme[26]. The birefringence is calculated as the difference of the stress components multiplied by C_m in the melt and by C_g in the glassy state. The birefringence at the glass transition in the respective node is stored and the increments below T_g are added to it.

EXPERIMENTAL

The investigated polymer was polycarbonate Makrolon CD 2000/15000 from Bayer AG, FRG ($\bar{M}_w \sim 20\,000$). The dynamic shear moduli G' and G'' in the melt were determined with a Rheometrics RVE-M plate–plate rheometer and a cone–plate rheometer. The complex moduli E^* and G^* in the glassy state were determined with a DMTA dynamic mechanical thermal analyser of Polymer Laboratories in bending and shearing mode, respectively. The linear expansion coefficient was measured with the aid of a Perkin–Elmer TMS-2 thermal mechanical analyser.

The stress-optical coefficient in the melt (C_m) was determined with a flow birefringence apparatus in a

* Engineering bureau SEPRA, Leidschendam, The Netherlands

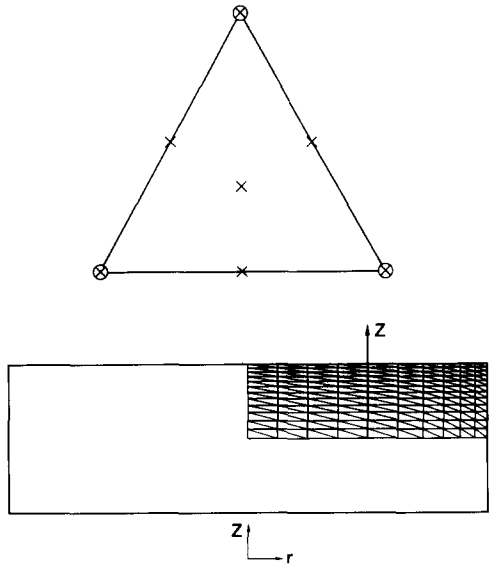

Figure 1 Seven-node Taylor–Hood element (above) and cross-section of the sample with the finite element grid (below); for symmetry reasons only one quarter is covered: (○) pressure, linear; (×) velocity and temperature, quadratic

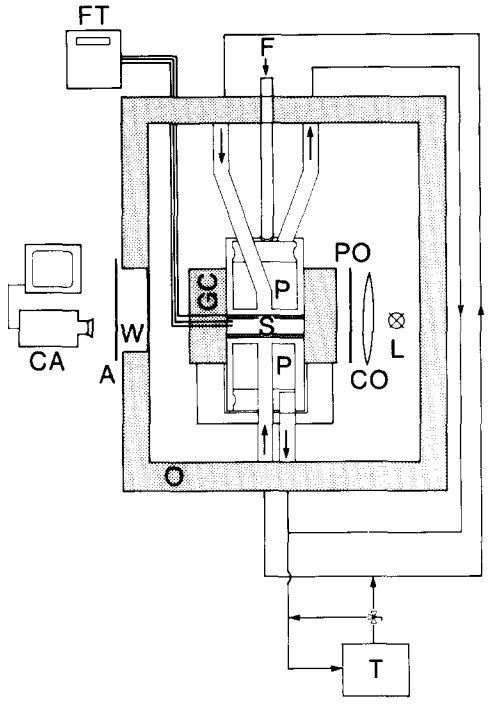

Figure 2 Quenching apparatus: A, analyser; CA, camera; CO, collimator; F, load; FT, fluoroptic thermometer; GC, quartz glass cylinder; L, light source; O, oven; P, piston; PO, polarizer; S, sample; T, thermostat pump; W, window

modified cone–plate arrangement as described in ref. 27 but with reversed light direction. In the glassy state the stress-optical coefficient C_g was determined in uniaxial extension on a micro-tensile tester placed on the turntable of a polarizing microscope. The stress-optical characterization will be published in more detail in due course.

Two types of quenching experiments were carried out. In the free-quenching experiment the prepressed samples, discs of typically 3 cm diameter, were annealed in an oven for several hours at 170°C and then dropped into a stirred NaCl solution of a given temperature (NaCl was added to match the density with that of the polymer). In the constrained-quenching experiment the sample of the same dimensions was placed between two pistons and a quartz cylinder, as shown in *Figure 2*. The whole set-up was then kept above T_g for several hours before, by opening a valve, thermostated water was pumped through the pistons. The temperatures of the cooling copper plates and the specimen were recorded during cooling with the aid of a Luxtron fluoroptic thermometer 750. After thermal equilibrium had been reached the samples were removed.

The frozen-in birefringence distributions were measured in 1 mm thick radial cross-sections cut out of the samples. The cutting surfaces were treated with a diamond mill to make them smooth and flat.

RESULTS AND DISCUSSION

Stress-optical behaviour

As already mentioned a detailed stress-optical characterization of PC will be published. Here only part of the results are shown to justify the stress-optical coefficients that are used in the numerical calculations. The isothermal stress-optical behaviour of PC is described by *Figure 3*. The birefringence is plotted *versus* the applied stress difference on a double logarithmic scale. The data at temperatures above T_g, obtained with the flow birefringence apparatus, fall on one line. Also the data obtained from the tensile tester well below T_g fall on a straight line. It can be seen that the linear stress-optical rule is observed above as well as below T_g (~ 139°C). The stress-optical coefficient is independent of temperature in the molten state within the measured range. C_m is 3.45×10^{-9} Pa^{-1}. This is significantly lower than the values published by Kang and White[28], who mentioned that some crystallinity might have affected their results. C_g is 8.9×10^{-11} Pa^{-1} at room temperature, which is slightly higher than the values published by Woebcken[29] and Lee *et al.*[17] and lower than the value of Azuma[30]. In the molten state PC behaves as a generalized Newtonian liquid in the applied range of shear stresses and temperatures, since X does not deviate significantly from 45°. Birefringence *versus* shear stress is a straight line. The results obtained around the glass transition are not included because of the time dependence, which is not yet included in our calculations.

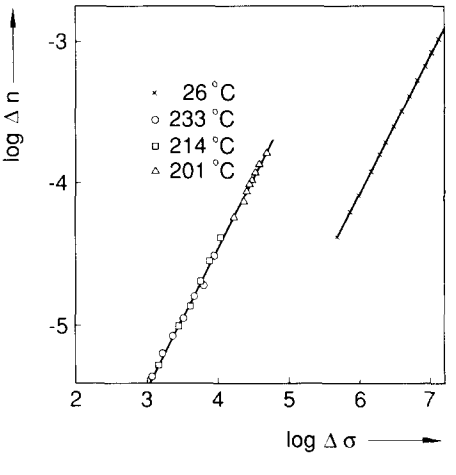

Figure 3 Birefringence Δn vs. applied stress difference $\Delta\sigma$ on a double logarithmic scale at different temperatures as indicated

Free quenching simulations

The input of our numerical program consists of the mesh (an example being shown in *Figure 1*), the boundary conditions for temperature and velocity, and the material properties. The mechanical and stress-optical properties of PC as used in our calculations are summarized in *Table 1*. As already mentioned a discontinuous step in properties at T_g is assumed. The values above and below T_g are extracted from our own measurements, except the compression modulus, which was derived from literature values[31].

For the residual birefringence not only the final state of stress is important but also the development of that state. This build-up is demonstrated in *Figures 4a* to *4d* for an example of a 1.2 mm thick disc, which was cooled at the free boundary from 160 to 100°C in 0.3 s. The distributions of the components of the stress tensor are drawn *versus* the z-direction for half of the thickness at a radial distance of $R/2$ from the axis, as indicated by the arrow in *Figure 1*. In *Figure 4a* the surface is still above the glass transition temperature, T_g. The stress in the radial direction is tensile at the surface and compressive in the core, σ_{zz} and σ_{rz} are zero over the whole thickness. The birefringence is proportional to σ_{rr}, since σ_{zz} is zero. As time develops, going from *Figure 4a* to *4d*, T_g penetrates from the surface towards the midplane of the disc, as indicated by the arrows. We see that the state of the stress at the solidifying front varies, taking also the different scales into account. It changes from tensile in *Figure 4b* to compressive in *Figure 4c*. Finally in *Figure 4d* an almost parabolic stress distribution is obtained. The tensile part of the final state of stress compares well with the result obtained with the aid of the analytical solution published by Struik[2] for a semi-infinite medium, as indicated in the figure. But the compressive stress at the surface is much higher in the analytical solution.

In *Figure 5a* the residual birefringence distribution as measured in the cross-section of a disc, which was quenched from 170°C down to room temperature, is compared with the result of the simulation. We see that the birefringence is predicted almost quantitatively without the use of any adjustable parameter. The interesting point is that the birefringence is not proportional to the stress difference in the rz-plane, shown in *Figure 5b*. The ratio of birefringence to stress difference in the core is smaller than that at the surface. This comes from the negative contribution of the compressive stress present at T_g to the total birefringence. This means that it is impossible to match the result by using a single stress-optical coefficient (i.e. that of the glassy state) as proposed in the literature. Owing to the contribution of frozen-in orientation induced by cooling stresses the birefringence distribution is not balanced although the stresses are.

Obviously the simple constitutive material description works well. The rubber-elastic behaviour above T_g is apparently quite realistic because of the high cooling rates, which quickly make the relaxation times very long. For higher initial temperatures a viscous model is included in the program. It turns out that much too high stresses and birefringence are predicted when the Newtonian viscosity with the measured WLF type[32] of temperature dependence is used down to T_g. This is understandable since a steady state, as described by viscosity, is never reached owing to the high rates.

We are aware that a viscoelastic model is the only realistic description of polymer behaviour. However, we do not expect that this will have a big influence on the results of a simulation of this kind of experiment. Only with slow cooling does stress relaxation become important. One unsolved problem is the choice of the appropriate T_g. It is well known that T_g is rate-dependent[32–36]. With the available techniques it is, however, not possible to measure T_g at cooling rates that compare with those in a quenching experiment. An extrapolation of e.g. two orders of magnitude does not

Table 1 Properties of PC as used in the calculations

Property	$T > T_g$	$T \leqslant T_g$
G (Pa)	1.5×10^6	895×10^6
α (K^{-1})	6.0×10^{-4}	2.0×10^{-4}
λ ($W\,m^{-1}\,K^{-1}$)	0.2	0.2
c_p ($W\,kg^{-1}\,K^{-1}$)	2.4×10^3	2.0×10^3
κ (Pa)	3.5×10^9	2.3×10^9
C (Pa^{-1})	3.45×10^{-9}	8.9×10^{-11}

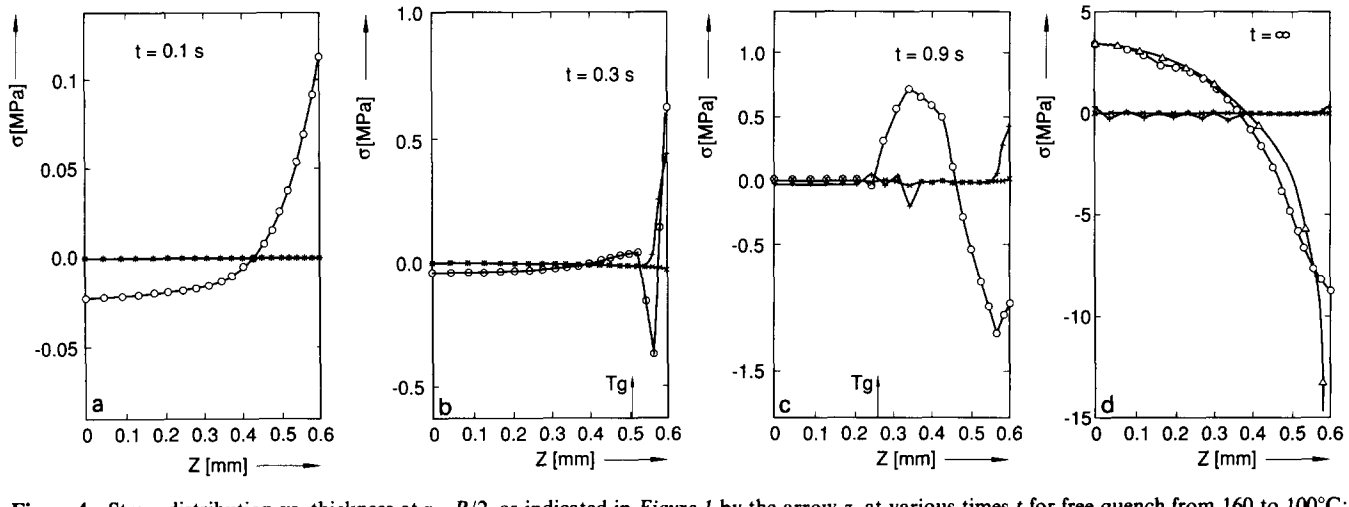

Figure 4 Stress distribution vs. thickness at $r = R/2$, as indicated in *Figure 1* by the arrow z, at various times t for free quench from 160 to 100°C: (○) σ_{rr}; (×) σ_{rz}; (+) σ_{zz}; (△) calculated with Struik's formula

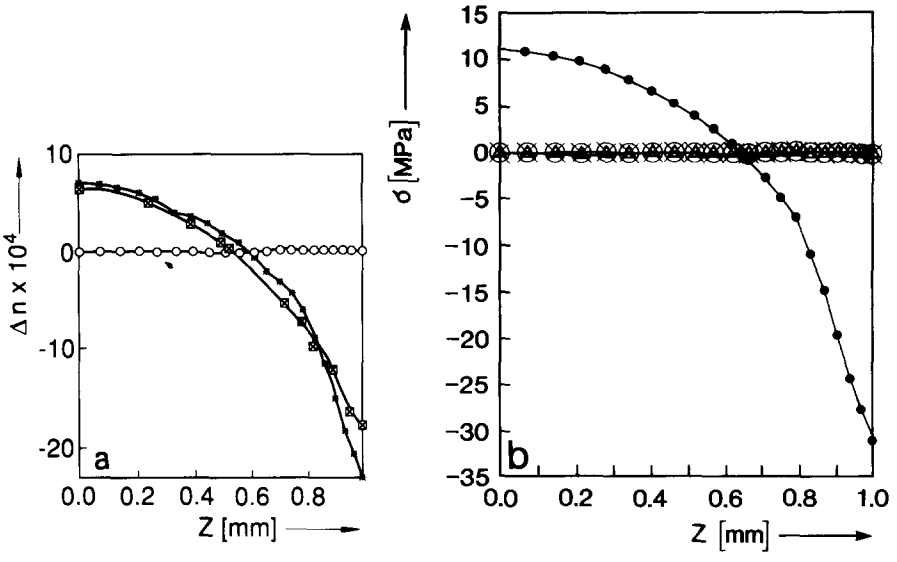

Figure 5 (a) Measured and calculated birefringence distribution vs. thickness at $r = R/2$ in free quench from 170 to 25°C: (○) $\Delta n_{r\phi}$; (+) Δn_{rz}; (×) $\Delta n_{\phi z}$; (⊠) measured Δn_{rz}. (b) Calculated stress distribution vs. thickness at $r = R/2$ in free-quench from 170 to 25°C: (●) σ_{rr}; (⊗) σ_{zz}; (△) σ_{rz}

seem to be safe enough. There is also the problem of the definition of T_g. It is, however, not the purpose of this paper to discuss this issue in more detail. The T_g used in the simulations was obtained from interpolation of the maxima of the first derivative of the d.s.c. heating and cooling scans at the highest achievable rate of 80 K min^{-1} on the Perkin–Elmer DSC-2.

Constrained quenching simulations

The presence of a wall changes the stress development during cooling drastically. Because of the adhesion between polymer and wall the stresses will not be equilibrated in the polymer. The thermal expansion coefficient of the polymer is in general considerably higher than that of the wall so that during cooling from thermal equilibrium only tensile stresses will be built up until the polymer is released from the wall. Therefore one can expect that the stresses at the glass transition will be higher so that the influence of the frozen-in orientation on the residual birefringence distribution will increase. The distribution of stresses and birefringence and the imbalance of the latter will, however, depend on the moment and method of release of the polymer from the wall.

In the simulation program the thermal expansion of the wall was disregarded, and symmetry was assumed with respect to the midplane of the sample, although in the experiment only the upper piston followed the shrinkage of the sample. The sample did not make contact with the quartz cylinder so that it is reasonable to assume adiabaticity at the rim. In the program either perfect adhesion to the cooling wall was prescribed or complete freedom. No friction coefficient was introduced.

As already mentioned the moment of release is very important. *Figures 6a* to *6c* show the calculated residual birefringence distributions in the cross-section for three different release times for a sample that was cooled from 170 to 25°C at a rate of 60°C s^{-1}. In *Figure 6a* the boundary was released just after the skin had become solid. The distribution is very similar to the one of free quenching. Only beyond the surface is the compressive stress flatter. In *Figure 6b* the sample was released after the solidification had reached the midplane. The birefringence is much lower and only positive. The result is affected by slight numerical instabilities. *Figure 6c* shows the result of the case where the release time was chosen so that the best fit with the measured distribution, which is also indicated in the figure, could be obtained. As one can see the fit is only reasonable. Obviously the release is more gradual than assumed in the calculations. In practice it will depend on the adhesion between the polymer and the wall and therefore also on the contamination of the surface. Also the thickness of the sample is important. From *Figure 6c* it can be concluded that in this case the release occurred before the solidification had reached the midplane.

This phenomenon certainly has implications for the calculation of residual stresses and orientation in injection-moulded parts, where a solid skin is formed already during injection under the influence of high pressure gradients. Simulation programs usually assume a no-slip condition.

While in the example shown for free quenching one might accept the error made by using a single 'adjustable' stress-optical coefficient, it is impossible to obtain a reasonable fit in this way in the constrained-quenched case, as one can conclude from *Figures 6a* to *6c*.

CONCLUSIONS

Polycarbonate is very suitable for the measurement of stress-induced birefringence because of its high positive stress-optical coefficient in the melt and in the glassy state.

The numerical program described is able to predict residual birefringence distributions in quenched PC specimens by making use of the linear stress-optical rule above and below T_g and freezing in the birefringence at T_g. The simple elastic constitutive relation gives satisfactory results for the simulation of the cooling at high rates.

The measured and calculated birefringence distributions are not balanced, since the stresses built up in the molten state induce orientation, which is frozen in at the glass transition. Therefore it is not possible to fit the

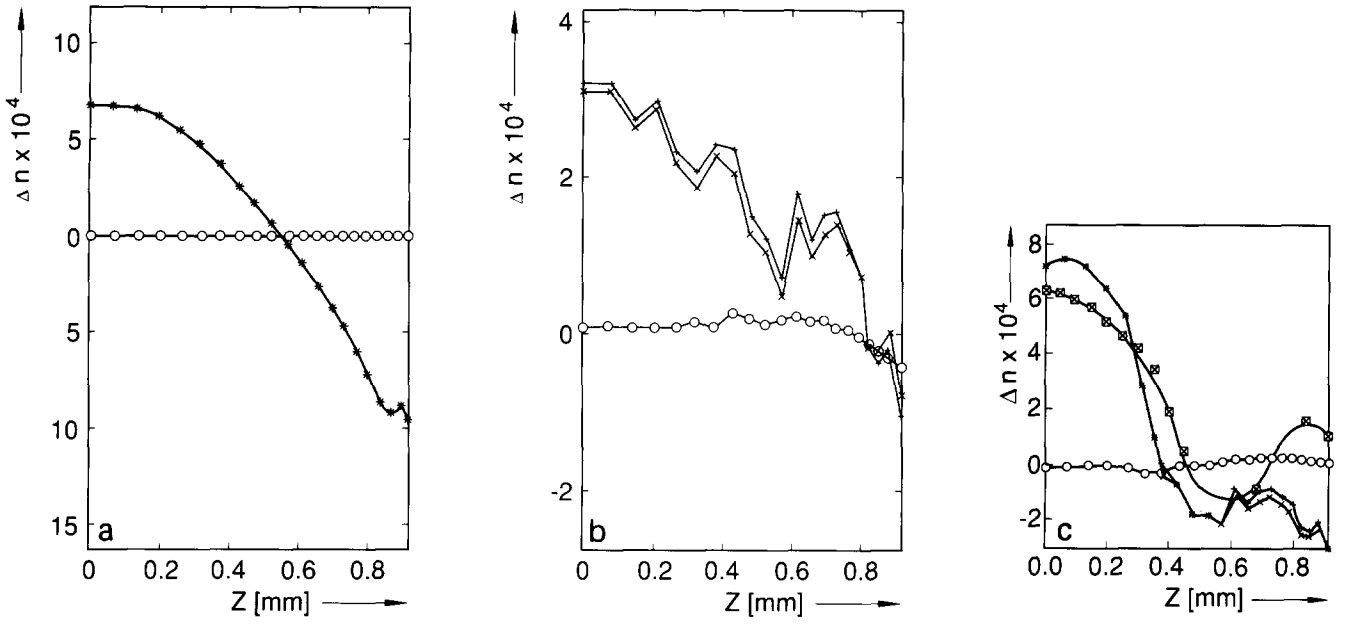

Figure 6 (a) Birefringence distribution vs. half of the thickness at $r=R/2$ in constrained quench, release time = 0.9 s: symbols as in *Figure 5a*. (b) As (a) but release time = 3.0 s. (c) As (a) but release time = 2.65 s; (⊠) measured Δn_{rz}

measured distributions with a single stress- or strain-optical coefficient. The incorporation of the stress-optical coefficient of the melt makes it possible to use the same model also for the calculation of flow-induced frozen-in birefringence in injection-moulding simulations.

By quenching between two solid walls, high tensile stresses are built up in the melt so that more orientation is frozen in. This leads to a flat birefringence distribution. Depending on the moment of release from the walls the flat part of the distribution will reach further towards the mid plane of the sample. It is possible to fit the measured birefringence by adjusting the moment of release in the simulation. It turns out that this release can occur before complete solidification of the sample but depends on the adhesion of the polymer on the walls. However, little or nothing is known about the adhesion during rapid cooling. We therefore intend to modify the cooling surfaces in such a way that we can learn more about this phenomenon experimentally, since we believe that it is of importance for the simulation of the injection-moulding process.

ACKNOWLEDGEMENT

The authors would like to express their thanks to Dr F. P. T. Baaijens for his help with the development of the numerical program.

LIST OF SYMBOLS

C	stress-optical coefficient
$\boldsymbol{D}^{\mathrm{d}}$	deviatoric rate of deformation tensor
E	Young's modulus
G	shear modulus
$\boldsymbol{I}$	unit tensor
R	radius
T_{r}	rubber temperature
T_{g}	glass transition temperature
c_p	specific heat
$\dot{e}$	differential internal energy
$\boldsymbol{h}$	heat flux density
Δn	birefringence
p	hydrostatic pressure
r	radial direction
$\boldsymbol{u}$	velocity
z	axial direction
θ	tangential direction
Γ	retardation
X	extinction angle
α	thermal volume expansion coefficient
η	viscosity
κ	compression modulus
λ	thermal conductivity
v	specific volume
v_0	specific volume at glass transition
$\boldsymbol{\sigma}$	stress tensor
σ_1	tensile stress
σ_{21}	shear stress
τ	deviatoric shear tensor
∇	nabla operator

REFERENCES

1 Struik, L. C. E., 'Physical Aging in Amorphous Polymers and Other Materials', Elsevier, Amsterdam, 1978
2 Struik, L. C. E. *Polym. Eng. Sci.* 1978, **18**, 799
3 Sitters, C., 'Numerical simulation of injection-molding', PhD Thesis, Techn. Univ. Eindhoven, 1988
4 Wang, V. and Hieber, C. SPE 46th Annual Techn. Conf., Atlanta, 1988, p. 290
5 Mavridis, H., Hrymak, A. N. and Vlachopoulos, J. *J. Rheol.* 1988, **32**, 639
6 Wales, J. L. S., van Leeuwen, J. and van der Vijgh, R. *Polym. Eng. Sci.* 1972, **12**, 358
7 Isayev, A. I. and Hieber, C. A. *Rheol. Acta* 1980, **19**, 168
8 Rudd, J. F. and Andrews, R. D. *J. Appl. Phys.* 1960, **31**, 818
9 Wales, J. L. S., 'The Application of Flow Birefringence to Rheological Studies of Polymer Melts', Delft University Press, 1976
10 Isayev, A. I. *Polym. Eng. Sci.* 1983, **23**, 271
11 Janeschitz-Kriegl, H., 'Polymer Melt Rheology and Flow Birefringence', Springer, Berlin, 1983
12 Janeschitz-Kriegl, H. *Adv. Polym. Sci.* 1969, **6**, 170
13 Aggarwala, B. D. and Saibel, E. *Phys. Chem. Glasses* 1961, **2**, 137
14 Greener, J. and Kenyon, P. M. *Proc. SPIE – Int. Soc. Opt. Eng.* 1981, **279**, 92

15 Lee, E. M., Rogers, T. G. and Woo, T. C. *J. Am. Ceram. Soc.* 1965, **48**, 480
16 Wust, C. J. and Bogue, D. C. *J. Appl. Polym. Sci.* 1983, **28**, 1931
17 Lee, S., de la Vega, J. and Bogue, D. C. *J. Appl. Polym. Sci.* 1986, **31**, 2791
18 Treuting, R. G. and Read, W. T. *J. Appl. Phys.* 1951, **22**, 130
19 So, P. and Broutman, L. J. *Polym. Eng. Sci.* 1976, **16**, 785
20 Haworth, B., Sandilands, G. J. and White, J. R. *Plast. Rubber Int.* 1980, **5**, 109
21 White, J. R. *Polym. Testing* 1984, **4**, 165
22 Saffell, J. R. and Windle, A. H. *J. Appl. Polym. Sci.* 1980, **25**, 1117
23 Mittal, R. K. and Rashmi, V. *Polym. Eng. Sci.* 1986, **26**, 310
24 Zienkiewicz, O. C., 'The Finite Element Method', 3rd Edn., McGraw-Hill, London, 1977
25 Soulaiman, A., Fortin, M., Ouellet, Y., Dhatt, G. and Bertrand, F. *Comp. Meth. Appl. Mech. Eng.* 1987, **62**, 47
26 Baaijens, F. P. T., in 'Flow Modelling in Industrial Processes' (Eds. A. W. Bush, B. A. Lewis and M. D. Warren), Ellis Horwood, Chichester, 1988
27 van Aken, J. A., Gortemaker, F. H., Janeschitz-Kriegl, H. and Laun, H. M. *Rheol. Acta* 1980, **19**, 159
28 Kang, H. J. and White, J. L. *Int. Polym. Processing* 1986, **1**, 1
29 Woebcken, W. *Kunststoffe* 1961, **51**, 547
30 Azuma, K. and Soezima, Y. *Jap. J. Appl. Phys.* 1967, **6**, 909
31 Zoller, P. *J. Polym. Sci., Polym. Phys. Edn.* 1982, **20**, 1453
32 Williams, M. L., Landel, R. F. and Ferry, J. D. *J. Am. Chem. Soc.* 1955, **77**, 3701
33 Ferry, J. D., 'Viscoelastic Properties of Polymers', 3rd Edn., Wiley, New York, 1980
34 Aklonis, J. J. *Polym. Eng. Sci.* 1981, **21**, 896
35 Chow, T. S. *Polym. Eng. Sci.* 1984, **24**, 1079
36 Ichihara, S., Komatsu, A. and Hata, T. *Polym. J.* 1971, **2**, 644